# Fractal to nonfractal behavior of vapor-deposited gold surfaces and the relationship to the substrate temperature

J. L. Zubimendi, M. E. Vela, R. C. Salvarezza, L. Vázquez,* J. M. Vara,† and A. J. Arvia
*Instituto de Investigaciones Fisicoquímicas Teóricas y Aplicadas (INIFTA), Casilla de Correo 16, Sucursal 4, (1900) La Plata, Argentina*
(Received 28 March 1994)

A transition from a fractal to a nonfractal surface behavior of thin gold films deposited at different substrate temperatures has been observed by scanning tunneling microscopy. At $T_s = 298$ K, columnar deposits are formed whereas at 673 K a faceted deposit is obtained. Data can be used to test the validity of different growth models, including surface atom relaxation.

PACS number(s): 81.15.−z, 82.20.Wt

Growth models for new solid phases, and the development of moving interfaces, are subjects of extensive theoretical investigations [1]. Recently, scanning tunneling microscopy (STM) [2–4] imaging data were used for the fractal characterization of gold film surfaces prepared by vapor deposition on a smooth glass at the growth rate $v = 30$ nm s$^{-1}$ and the substrate temperature $T_s = 298$ K. From these studies [2–4] it has been concluded that the surface of these films behaves as a self-affine fractal with a roughness exponent $\alpha \cong 0.90$ for $L < d_s$, and $\alpha \cong 0.36$ for $L > d_s$, where $L$ is the scan length and $d_s$ is the average columnar size. The value $\alpha \cong 0.36$ was consistent with the predictions of the stochastic growth model of Kardar, Parisi, and Zhang (KPZ) [5] and different atomistic growth models [1]. However, the self-affine fractal surface characteristics of those films was due to height fluctuations of columns rather than atoms, as predicted by atomistic models [1]. On the other hand, for $L < d_s$, $\alpha \cong 0.9$ indicated smooth textured columnar surfaces which resulted from the surface mobility of gold atoms, leading to the disappearance of irregularities within a diffusion length close to $d_s$ [2–4]. In this case, the $\alpha$ value exceeds that expected for continuum models incorporating surface relaxation [6], although it is consistent with the $\alpha$ value derived for simple growth models in which particles are randomly deposited onto a substrate, and subsequently they relax to kink sites maximizing the number of saturated bonds [7,8]. However, the model presented in [6] attempts to explain the interface growth at high temperatures, where relaxation of incident atoms via rapid surface diffusion plays a relevant role in producing a smooth growth. Then, in order to test the validity of the different models, experimental data about the self-affine fractal characteristics of growing interfaces covering a wide $T_s$ range are needed.

This paper reports the influence of $T_s$ and $v$ on the self-affine character of vapor-deposited gold film surfaces grown in the 298 K $< T_s <$ 673 K range, from the analysis of STM images. In this $T_s$ range, gold atom surface diffusion plays a relevant role in determining the growth mode of gold films [9]. Results show that the decrease in $v$ from 30 to 0.1 nm s$^{-1}$ at $T_s = 298$ K produces no marked changes in the surface properties of columnar structured gold deposits. Conversely, the increase in $T_s$ from 298 to 673 K leads to the disappearance of the columnar structure with $\alpha \cong 0.4$, and to the formation of a smooth textured faceted gold surface with $\alpha \cong 0.9$.

Gold deposits were grown in an evaporator chamber on smooth glass substrates previously cleaned in an ultrasonic bath by sequentially using water, trichloroethylene, acetone, and ethanol [2–4]. The maximum deviation between the direction of incident particles and the substrate normal was 9°, and the experimental conditions at the evaporator chamber were pressure $P = 10^{-4}$ torr, average deposit growth rate $\langle v \rangle = 0.1$ nm s$^{-1}$, and 298 K $< T_s <$ 673 K. The average film thickness as estimated by the weight method was $\langle h \rangle \cong 200$ nm. Previous results for this system [3] showed that for $\langle h \rangle > 170$ nm the root-mean-square roughness of the deposit surface approached a steady state.

A McAllister STM operating in air was used to study the surface morphology of gold deposits. The STM was calibrated by imaging highly oriented pyrolytic graphite (HOPG). Tips were made from 0.25-mm-diameter platinum-iridium wires directly by cutting. Although different tips were used to minimize occasional tip geometric artifacts, no influence of the tip shape on our experimental data was found. STM measurements were made using a 0.05-V bias voltage with the tip (+), at 1–2 nA constant current. Data were acquired in a fully automated work station and stored as digitized images with 200×200 pixels. Occasionally, images with 400×400 pixels were taken with similar results.

Usually STM measurements involve an uncertainty about whether the tip scans over a parallel or a tilted

*Also at Instituto de Ciencia de Materiales, Consejo Superior de Investigaciones Científicas, Departamento de Física Aplicada C-XII, Universidad Autónoma de Madrid, Madrid, Spain.
†Also at Departamento de Química Física Aplicada C-II, Universidad Autónoma de Madrid, 28049 Madrid, Spain.

 

plane of the sample. The presence of a tilted plane introduces an overestimation in the value of $\alpha$, as results from computer-generated surfaces with added planes. STM plane removal options in the software have been used successfully to remove the tilted plane [10]. Therefore, in this paper STM data are presented after the instrument's plane fitting and subtracting procedure [2].

STM images of vapor-deposited gold film surfaces resulting from those runs made at $v=0.1$ nm s$^{-1}$ and $T_s=298$ K [Fig. 1(a)] show rounded top columns which are $d_s \cong 20$ nm in average size, and branched voids. The cross sections of all these STM images [Fig. 1(a) and 1(b)] correspond to jagged profiles due to the height fluctuations of columnar elements. STM images of vapor-deposited gold surfaces prepared at $T_s=298$ K and $v=30$ nm s$^{-1}$ show a similar surface structure, as already reported [2–4].

Runs made at $T_s=473$ K and $v=0.1$ nm s$^{-1}$ result in a complex gold surface structure in which both columnar and faceted domains can be simultaneously imaged [Fig. 2(a)]. These faceted gold crystals of about 60–75-nm average size are formed by small elements 15–20 nm in average size [Fig. 2(b)]. These faceted domains are embedded in columnarlike domains. Evidently, at $T_s=473$ K, irregular (columnar) and regular (faceted) phases coexist. At $v=0.1$ nm s$^{-1}$ the relative contribution of columnarlike domains again decreases when $T_s$ is set to 573 K.

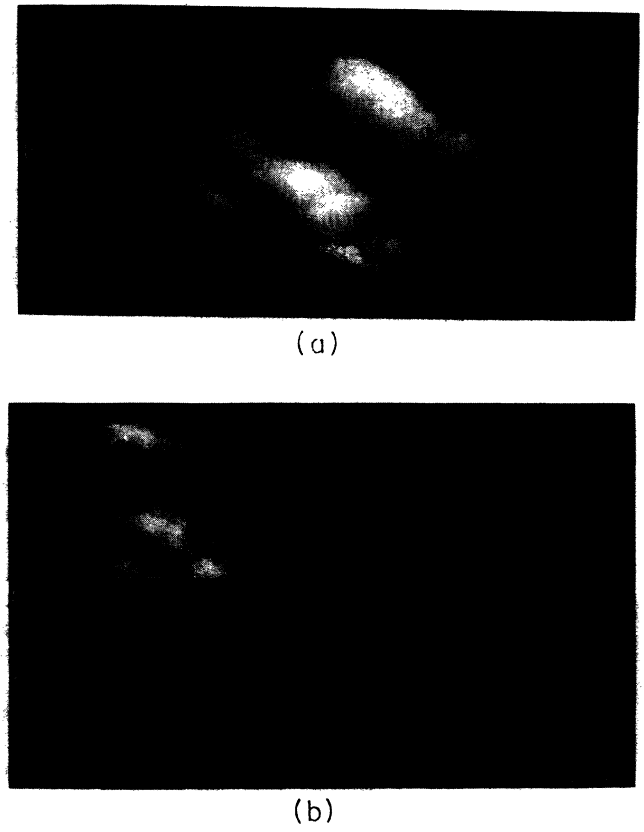


FIG. 1. STM image of a vapor-deposited gold film grown at $v=0.1$ nm s$^{-1}$ and $T_s=298$ K. (a) Three-dimensional (3D) image. (b) Cross section of the image shown in (a).

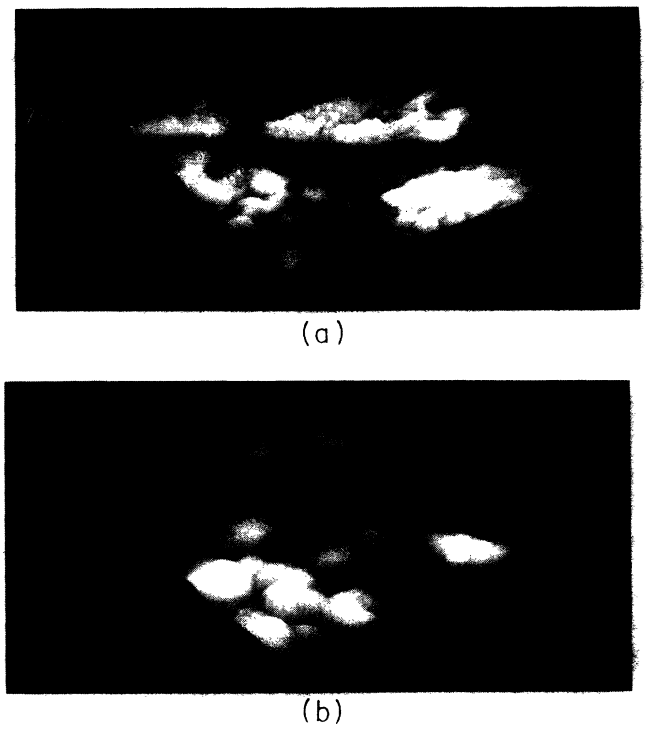


FIG. 2. 3D STM images at different scales of a vapor-deposited gold film grown at $v=0.1$ nm s$^{-1}$ and $T_s=473$ K.

In this case, large gold facets 100–150 nm in average size are formed, presumably by a coalescence mechanism initially involving small tip columns.

Finally, for $v=0.1$ nm s$^{-1}$ and $T_s=673$ K, STM images show that the columnarlike structure is practically suppressed [Fig. 3(a)], and the surface topography is dominated by large gold facets. The cross section of these facets, as derived from STM images [Fig. 3(b)], show profiles with a smooth texture [11], although some bumps related to defects on the facets can be observed. As the large scale deterministic variation of the surface was eliminated, the smooth texture of the deposit results from the surfaces of the gold crystals.

The analysis of surface profiles resulting from the above-mentioned data was based on the dynamic scaling method. Accordingly, the properties of these interfaces and the roughness generated by different models scale as

$$\xi(L,h) \propto L^{\alpha} f(x) , \tag{1}$$

where $L$ is the sample size, $\alpha$ is the characteristic roughness exponent, $f(x)=\langle h \rangle / L^{\gamma}$, $f(x)=$const for $x \Longrightarrow \infty$, $f(x)=x^{\alpha/\gamma}$ for $x \Longrightarrow 0$, and $\xi$ is defined as

$$\xi(L)=\left[(1/N)\sum_i [h(x_i)-\langle h \rangle]^2\right]^{1/2} , \tag{2}$$

where $h(x_i)$ is the deposit height measured along the $x$ direction at the point $x_i$, and $\langle h \rangle$ is the average height of the sample formed by $N$ points. After a certain critical time or thickness is reached, (1) becomes

$$\xi(L) \propto L^{\alpha} . \tag{3}$$

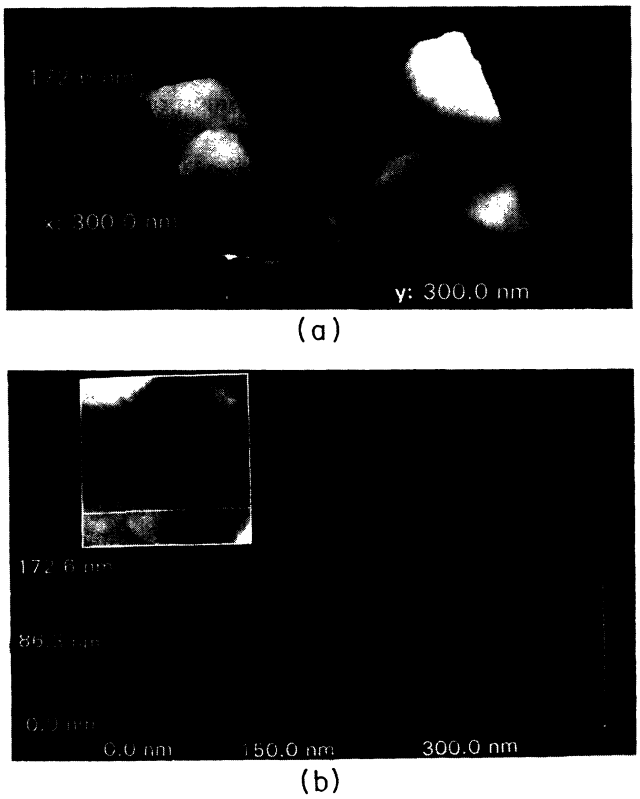


FIG. 3. STM images of a vapor-deposited gold film grown at $v=0.1$ nm s$^{-1}$ and $T_s=673$ K. (a) 3D image. (b) Cross section of the image depicted in (a).

The STM images presented in this paper show that at $T_s=298$ K, the decrease in $v$ from $v=30$ to 0.1 nm s$^{-1}$ results in similar columnar structures. Thus for $v=0.1$ nm s$^{-1}$ the $\log_{10}\xi$ vs $\log_{10}L$ plots exhibit two straight lines with a crossing point at $\log_{10}\xi_{STM}=0.6$ and $\log_{10}L=1.6$, and a saturation region at $\log_{10}L>2.6$ [Fig. 4(a)]. The slope of the straight lines is $\alpha(I)=0.71\pm0.07$ for $\log_{10}L<1.6$, and $\alpha(II)=0.41\pm0.06$ for $L_s>1.6$, respectively. It should be noted that although for computer simulated fractals data covering four to five orders of magnitude are required for logarithmic fitting, for experimental systems the situation is less ambitious and log vs log linear plots covering at least one order of magnitude or thereabouts are accepted.

As already reported [3], the capability of this method was verified by analyzing several computer-generated self-affine fractal surfaces with preset values of $\alpha(\alpha_{th})$ built on $200\times200$ and $256\times256$ square grids by using the successive random addition algorithm [12]. A good agreement between the measured $\alpha_m$ and $\alpha_{th}$ was found in the $0.2<\alpha_{th}<0.6$ range, whereas $\alpha_m$ becomes smaller than $\alpha_{th}$, the magnitude of the deviation increasing with $\alpha_{th}$, for $\alpha>0.6$. A better agreement of data can be obtained by increasing substantially the number of points in the square grid, for instance $1000\times1000$ pixels. However, the $200\times200$ grid involves a short imaging time, minimizing drift effects. Thus the $\alpha_m$ vs $\alpha_{th}$ plot was used to correct the $\alpha$ values measured with the STM method. Then $\langle\alpha(I)\rangle$ and $\langle\alpha(II)\rangle$, the averaged values after correction, resulting from 20 different STM images with $L$ between 20 and 550 nm, are $\langle\alpha(I)\rangle=0.90\pm0.07$ and $\langle\alpha(II)\rangle=0.40\pm0.05$. These values are in good agreement with those obtained for $v=30$ nm s$^{-1}$ [2–4]. Therefore, no marked influence of $v$ on the gold surface topography could be observed within the $v$ range covered in this work.

The $\log_{10}\xi$ vs $\log_{10}L$ plots for the deposits grown at $T_s=673$ K and $v=0.1$ nm s$^{-1}$, i.e., those films which exhibited a predominantly faceted topography, lead to a straight line with $\alpha\cong0.77\pm0.07$, and a saturation region close to the image size [Fig. 4(b)]. The average value of $\langle\alpha\rangle$ after correction [3], resulting from the analysis of 20 STM images with $L$ between 20 and 550 nm, is $\langle\alpha\rangle=0.90\pm0.07$. It should be noted that for $T_s=673$ K, the rms value increases by a factor of three as compared to that derived from the sample grown at $T_s=298$ K, due to the predominantly smooth profiles of the large gold facets.

Sometimes saturation regions such as those observed in Figs. 4(a) and 4(b) close to the image size were observed

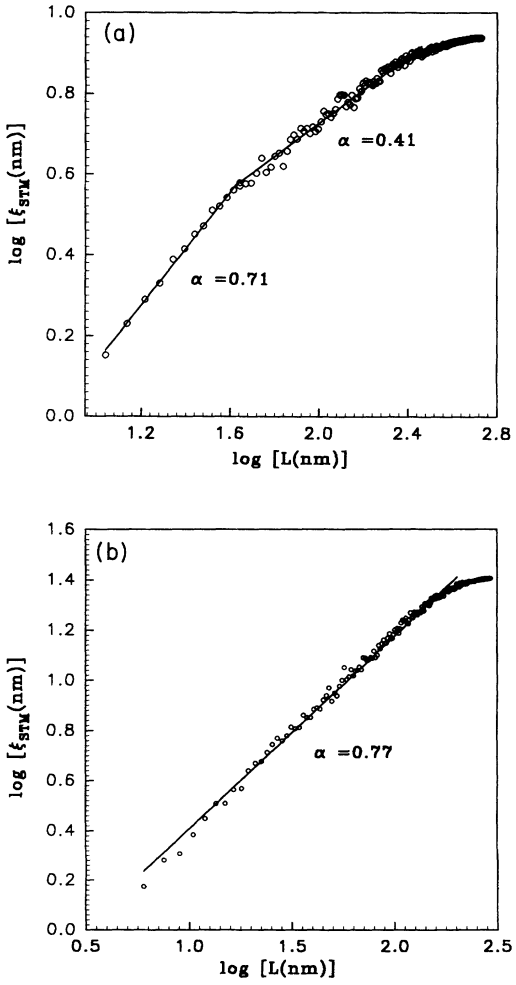


FIG. 4. $\log_{10}\xi_{STM}$ vs $\log_{10}L$ plot from gold films grown at $v=0.1$ nm s$^{-1}$ and different substrate temperatures ($T_s$). (a) $T_s=298$ K. (b) $T_s=673$ K.

when the computer-generated self-affine fractal surfaces were analyzed by this method. Thus, in principle, this region could be an artifact, although the existence of an outer cutoff is evident as these films appear as completely smooth ($\alpha=0$) when imaged by scanning electron microscopy.

The characteristics of the $\log_{10}\xi$ vs $\log_{10}L$ plots for gold deposits grown in the 473 K $< T_s <$ 573 K range and $v=0.1$ nm s$^{-1}$, i.e., those films where both faceted and columnar topography are present, depend on whether the image analysis is focused on either the faceted or columnar domains. Thus for faceted domains straight lines in the $\log_{10}\xi$ vs $\log_{10}L$ plot are accomplished with $\langle\alpha\rangle\cong 0.90\pm 0.07$, whereas for columnar domains two straight line ranges in the $\log_{10}\xi$ vs $\log_{10}L$ plot with $\langle\alpha(I)\rangle\cong 0.9$ and $\langle\alpha(II)\rangle\cong 0.4$, respectively, are observed.

For those vapor-deposited gold films grown in the 298 K $< T_s <$ 673 K range, similar $\langle\alpha\rangle$ values were obtained by estimating $\xi_s$, the average value of the root-mean-square roughness for each STM image, from relationship [4]

$$\xi_s \propto S^{\alpha} , \tag{4}$$

where $S$ is the image size.

The preceding $\langle\alpha\rangle$ values were confirmed by using $G(L,t)$, the height-to-height correlation function, resulting from the analysis of STM images [1]. In this case, the following equations were used to evaluate $\alpha$:

$$G(L)=\left[(1/N)\sum_i [h(x_i)-h(x_0)]\right]^2 \tag{5}$$

and

$$G(L)\propto L^{2\alpha} . \tag{6}$$

Again, $\langle\alpha\rangle$ values derived in this way are in good agreement with those obtained by other methods.

From the above analysis it is clear that there is a transition in the growth mode of vapor-deposited gold film on glass which depends strongly on $T_s$. This fact should be related to the role of surface restructuring in the topography of aggregates, which has been studied extensively from computer simulations of different atomistic and continuum models [5–8].

The experimental results obtained in this work at $T_s < 0.5T_m$, where $T_m$ is the melting temperature, i.e., a temperature value where bulk diffusion is negligible and surface diffusion dominates [9], provide clear evidence about the role of surface diffusion in ordering growing surfaces. Accordingly, the disordered structure characterized by $\alpha\cong 0.4$ tends to disappear by increasing the temperature from 298 to 643 K, leading to a better-ordered structure with $\alpha\cong 0.9$.

The experimental results can be interpreted by using Villain's equation [13]:

$$(\partial h/\partial t)=v\nabla^2 h+\lambda(\nabla h)^2+K\nabla^2(\nabla^2 h) +\sigma\nabla^2(\nabla h)^2+F+\eta , \tag{7}$$

where $F$ is the net deposition flux, and $\eta$ is the $\delta$-function-correlated noise. The $v$- and $\lambda$-containing terms appear when desorption is operative [14]. The $v$-containing term is related to the surface tension [1], and the $\lambda$-containing term to the dependence of growth rate on the local tilt ($\lambda$) [15], whereas the $K$- and $\sigma$-containing terms are related to surface diffusion [14]. Note that for $K=0$ and $\sigma=0$, Eq. (7) leads to the KPZ equation [5].

When surface diffusion becomes irrelevant, Eq. (7) leads to the roughness exponent $\langle\alpha(II)\rangle\cong 0.4$, predicted by KPZ. On the other hand, when surface diffusion is operative, $K$ and $\sigma$ are nonzero, and crossover phenomena may occur as observed at low $T_s$ ($T_s=298$ K). In the limit of high temperatures ($T_s=673$ K) models presented in Refs. [6–8] can be used to describe the surface topography. The continuum model incorporating surface relaxation [6] developed for the molecular beam epitaxial growth at high temperature fulfills the following equation:

$$(\partial h/\partial t)=v\nabla^4 h+\lambda\nabla^2(\nabla h)^2+\eta , \tag{8}$$

which leads to $\alpha=\frac{2}{3}$ in three dimensions (3D) rather than $\alpha\cong 0.9$, as obtained from the experimental data at high $T_s$. On the other hand, in 3D a value of $\langle\alpha\rangle\cong 1$ is predicted by the growth model presented in [7], whereas the model presented in [8] leads to intermediate values, and in generic cases the system shows either a completely smooth surface ($\alpha=0$) or $\alpha=1$ [16].

The value $\alpha\cong 0.9$ means that the restructuring processes may be too strong to remove all surface irregularities, yielding large facets with a smooth texture. However, for high $T_s$ and $t\Longrightarrow\infty$ the growth of the faceted crystals could lead to a completely smooth surface. Thus for high $T_s$ the $\alpha=0.9$ value can be assigned to a transient regime of the growing surface, and a crossover to the Edwards-Wilkinson scaling [17] ($\alpha=0$) could be expected.

This work was financially supported by the Consejo Nacional de Investigaciones Científicas y Técnicas of Argentina (CONICET) and the CONICET-CSIC, Consejo Superior de Investigaciones Científicas of Spain, scientific cooperation agreement.

[1] F. Family, Physica A **168**, 561 (1990) and references therein.

[2] R. C. Salvarezza, L. Vázquez, P. Herrasti, P. Ocón, J. M. Vara, and A. J. Arvia, Europhys. Lett. **20**, 727 (1992).

[3] L. Vázquez, R. C. Salvarezza, P. Herrasti, P. Ocón, J. M. Vara, and A. J. Arvia, Appl. Surf. Sci. **70-71**, 413 (1993).

[4] P. Herrasti, P. Ocón, L. Vázquez, R. C. Salvarezza, J. M. Vara, and A. J. Arvia, Phys. Rev. A **45**, 7440 (1990).

[5] M. Kardar, G.Parisi, and Y. C. Zhang, Phys. Rev. Lett. **56**, 889 (1986).

[6] Z. W. Lai and S. Das Sarma, Phys. Rev. Lett. **66**, 2348 (1991).
[7] S. Das Sarma and P. Tamborenea, Phys. Rev. Lett. **66**, 325 (1991).
[8] D. Wolf and J. Villain, Europhys. Lett. **13**, 389 (1990).
[9] H. P. Bonzel, in *Surface Physics of Materials,* edited by J. M. Blakely (Academic, New York, 1975), p. 280.
[10] J. Krim, I. Hevaert, C. Haesendock, and Y. Bruynseraede, Phys. Rev. Lett. **70**, 57 (1993).
[11] J. Krim and J. O. Indekeu, Phys. Rev. E **48**, 1576 (1993).
[12] R. Voss, in *Fundamental Algorithms in Computer Graphics,* edited by R. A. Earnshaw (Springer-Verlag, Berlin, 1985).
[13] J. Villain, J. Phys I **1**, 19 (1991).
[14] D. D. Vvdensky, A. Zangwill, C. N. Luse, and M. R. Wilby, Phys. Rev. E **48**, 852 (1993).
[15] Z. W. Amar and F. Family, Phys. Rev. E **47**, 1595 (1993).
[16] M. Schroeder *et al.*, Europhys. Lett. **24**, 563 (1993).
[17] S. F. Edwards and D. R. Wilkinson, Proc. R. Soc. London Ser. A **381**, 17 (1982).

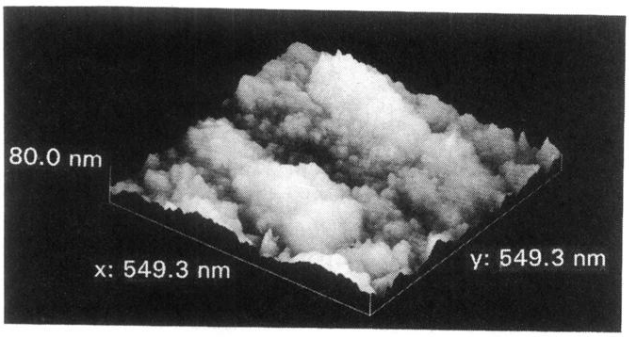


(a)

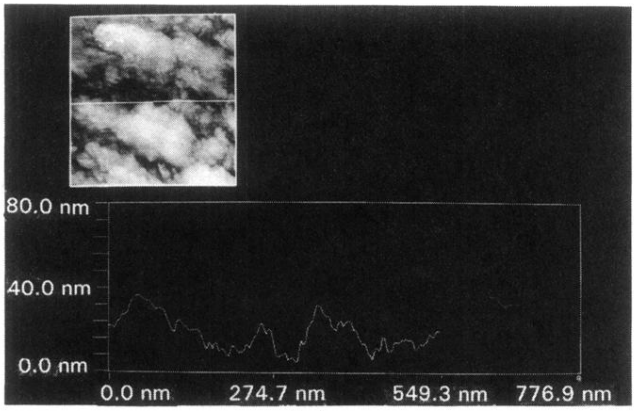


(b)

FIG. 1. STM image of a vapor-deposited gold film grown at $v = 0.1$ nm s$^{-1}$ and $T_s = 298$ K. (a) Three-dimensional (3D) image. (b) Cross section of the image shown in (a).

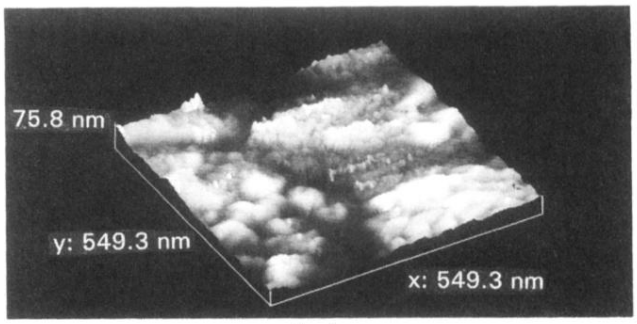


(a)

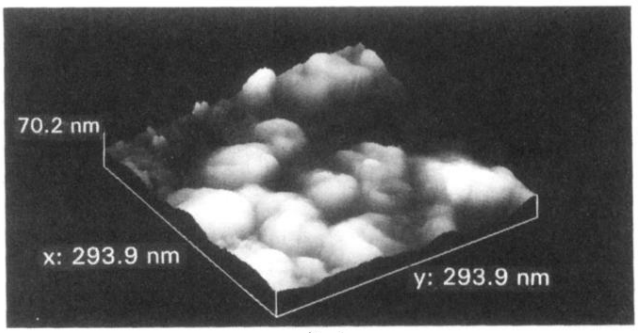


(b)

FIG. 2. 3D STM images at different scales of a vapor-deposited gold film grown at $v = 0.1$ nm s$^{-1}$ and $T_s = 473$ K.

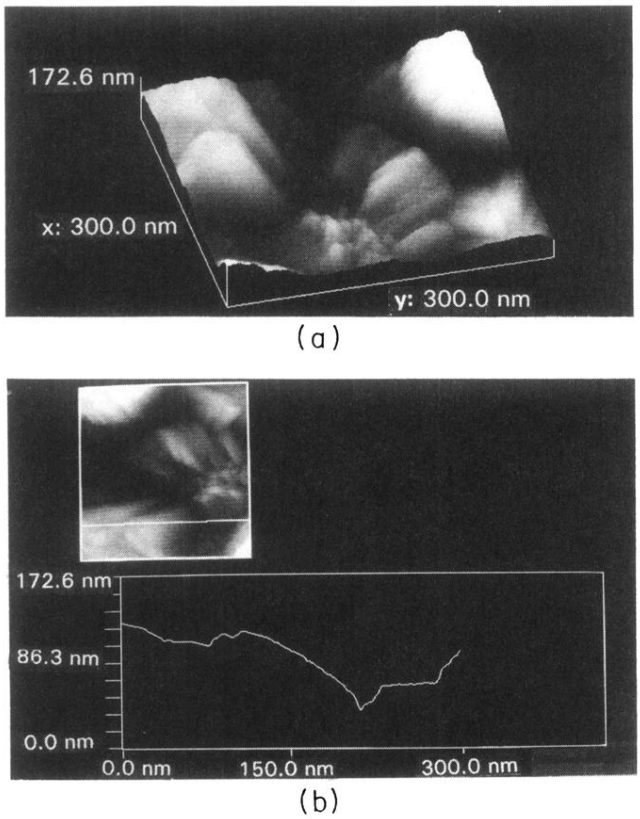


FIG. 3. STM images of a vapor-deposited gold film grown at $v = 0.1$ nm s$^{-1}$ and $T_s = 673$ K. (a) 3D image. (b) Cross section of the image depicted in (a).